



Environmental effects on antibiotic adsorption by Fe/Mn-loaded amphoteric clay

Zhi-feng Liu^{a,b}, Wen-bin Li^{c,*}, Qian Liang^{c,*}, Xun Fang^a, Hong-yan Deng^c

^aSchool of Chemistry and Environmental Science, Shaanxi University of Technology, Hanzhong, Shaanxi 723001, China, emails: lzhi-feng2005@163.com (Z.-f. Liu), 1967996969@qq.com (X. Fang)

^bState Key Laboratory of Qinba Bio-Resource and Ecological Environment, Shaanxi University of Technology, Hanzhong, Shaanxi 723001, China

^cCollege of Environmental Science and Engineering, China West Normal University, Nanchong Sichuan 637009, China, Tel. +86 08172568646; emails: lwb062@163.com (W.-b. Li), 2495055687@qq.com (Q. Liang), dhongyan119@163.com, (H.-y. Deng)

Received 27 January 2022; Accepted 27 May 2022

ABSTRACT

The environmental effects of Fe/Mn modification on antibiotic adsorption by amphoteric clay was explored using dodecyl dimethyl betaine (BS)-modified diatomite (D) and bentonite (B), which were prepared with the wet method and named BS-12 modified D (BS-D) and BS-B, respectively. Then, Fe-BS-D, Mn-BS-D, Fe/Mn-BS-D, Fe-BS-B, Mn-BS-B, and Fe/Mn-BS-B were prepared by modifying BS-D and BS-B with Fe²⁺ (prepared with FeSO₄·7H₂O) and Mn²⁺ (prepared with MnSO₄·H₂O). With D and B as controls, the environmental effects of different modified clays on the adsorption of chlortetracycline (CTC), oxytetracycline (OTC), and tetracycline (TC) were studied using the batch method, and the isothermal and thermodynamic characteristics of different modified clays for antibiotic adsorption were compared under optimum environmental conditions. The following results were obtained: (1) When the pH changed from 1 to 9, the amount of antibiotics adsorbed by each test sample increased first and then decreased, and the maximum amount was obtained at pH 5. With the increase in ionic strength, the amount of antibiotics adsorbed by each test sample decreased in a range of 0.01–0.5 mol/L. (2) The amount of adsorbed antibiotics in each test sample showed a positive temperature effect in a range of 10°C–40°C. The adsorption of antibiotics on different tested samples was spontaneous, endothermic, and entropy increasing. (3) The adsorption of TC, CTC, and OTC by the tested samples was described well by the Langmuir model. The maximum adsorption amount of antibiotics was in the range of 1.86–30.26 mol/kg, and ranked in the order of OTC > CTC > TC. (4) The pH of materials played a key role in the determination of the adsorption effect of antibiotics on different tested samples.

Keywords: Amphoteric clay; Fe/Mn modification; Adsorption amount; Antibiotic; Environmental factor

1. Introduction

The rapid development of aquaculture in China has contributed to antibiotics pollution that presents a serious hidden danger to agricultural production [1–3]. Therefore, the remediation and treatment of antibiotic pollution has become a focus of research and attracted considerable

interest worldwide [4,5]. Remediation materials have high adsorption capacities for antibiotics, and the modification of materials can improve the adsorption capacities of materials for antibiotics [6–8], so remediation material screening and material modification are of great importance to antibiotic pollution remediation and sustainable agricultural development.

* Corresponding authors.

In recent years, material adsorption has become a major subject of interest in pollution remediation research because of its simple operation, low cost, and obvious effects [9–11]. Modification by amphoteric surfactants can enhance the adsorption capacities of materials for heavy metals and organic pollutants [12,13]. The hydrophilic groups of amphoteric surfactants have positive and negative charges, so amphoteric modified materials can adsorb heavy metals and organic pollutants simultaneously [14]. Clay modified by dodecyl dimethyl betaine (BS-12) exhibits greatly enhanced ability to hydrophobically bind to organic pollutants, and its adsorption mechanism is mainly hydrophobic adsorption [15–17]. However, the adsorption ability of organic pollutants for single amphoteric modified clay is affected by modifier content. The adsorption capacity of amphoteric modified clay for organic pollutants can be improved by modifying amphoteric modified clay with other modifiers.

Iron and manganese have high elemental abundance in the first transition system, and they are among the most active and important geochemical elements [18]. Iron- and manganese-based metal oxides have the advantages of large specific surface areas, good pore structures and abundant surface active functional groups, which play an important role in the adsorption of organic and inorganic pollutants in the environment [19–22]. Du et al. [23] use different types of MnO_2 -modified diatomite to remove Cr^{6+} , and the maximum adsorption capacity reached 101 mg/g. Khraisheh et al. [24] used manganese-modified diatomaceous soil to adsorb heavy metals in sewage, and the specific surface area of diatomaceous soil loaded with manganese oxide increased 2.4 times, and the adsorption capacity reached its maximum when manganese oxide was loaded at 60.0 mg/g (diatomaceous soil). The loading of iron and manganese and amphoteric modification of materials improve the ability of the materials to adsorb pollutants. If Fe and Mn oxides are loaded again on the basis of amphoteric modification of clay, the adsorption capacity of a composite-modified clay for pollutants will be greatly enhanced. However, reports on the adsorption of pollutants on amphoteric clay loaded by iron and manganese are few to date.

In this study, iron and manganese were loaded on two different amphoteric clays, and the adsorption characteristics of three antibiotics under different environmental factors: temperature, pH, and ionic strength (I) were studied. In addition, the isothermal and thermodynamic characteristics of different modified samples for antibiotic adsorption were compared under optimum environmental conditions. The aim was to provide a reference for the use and testing of composite-modified clay in pollution remediation.

2. Materials and methods

2.1. Experimental materials

Diatomite (D, particle size of 325 mesh) was purchased from Chifeng City, China, and bentonite (B, particle size of 400 mesh) was purchased from Xinyang City, China. D and B were all purified with the washing method before use [25]. BS-12 was used as an amphoteric modifier (AR, Produced by Tianjin Xingguang Auxiliary Factory, Tianjin City, China).

$\text{FeSO}_4 \cdot 7\text{H}_2\text{O}$ (AR) and $\text{MnSO}_4 \cdot \text{H}_2\text{O}$ (AR) were purchased from ChengDu KeLong Chemical Reagent Factory, Chengdu City, Sichuan Province, China. Chlortetracycline (CTC), oxytetracycline (OTC), and tetracycline (TC) were purchased from Shanghai Aladdin Biochemical Technology Co., Ltd., China and had a purity of 99.9%.

2.2. Experimental design

2.2.1. Preparation of amphoteric clay

The BS-12 modified D (BS-D) and BS-12 modified B (BS-B) were prepared using the wet method [15]. The specific steps were as follows: BS-12 solution was added to 10 g of purified D or B (the mass ratio between the solution and soil was 10:1). The resulting solution was reacted for 6 h at 40°C, centrifuged at 4,800 rpm for 10 min, washed three times with deionized water (dH_2O), dried, ground, and sieved through a 60-mesh nylon sieve. The amount of BS-12 modifier was defined by Eq. (1):

$$W = m \times \text{CEC} \times M \times 10^{-6} \times \frac{R_{\text{BS}}}{C_{\text{BS}}} \quad (1)$$

where W is the mass (g) of BS-12; m is the mass (g) of B (or D); CEC is the cation exchange capacity of B (or D) (mmol/kg); M is the relative molar mass of BS-12 (g/mol); R_{BS} is the modification ratio of BS-12; and C_{BS} is the content (mass fraction) of BS-12.

2.2.2. Preparation of Fe/Mn-loaded amphoteric clay

Approximately 30.00 g of BS-D (or BS-B) was dispersed in 4 mol/L sodium hydroxide (NaOH) solution with solid-liquid ratio of 1:3 and stirred in a water bath at constant temperature (90°C) at 150 rpm speed for 2 h. Then, 250 mL of 1 mol/L $\text{MnSO}_4 \cdot \text{H}_2\text{O}$ (or $\text{FeSO}_4 \cdot 7\text{H}_2\text{O}$) solution was added to the mixture. The resulting solution was fully stirred for 1 h and left to stand at room temperature for 24 h. The samples were separated. Approximately 250 mL of 1 mol/L $\text{FeSO}_4 \cdot 7\text{H}_2\text{O}$ (or $\text{MnSO}_4 \cdot \text{H}_2\text{O}$) solution was added. The above operation was repeated. After centrifugation at 4,800 rpm for 20 min, the samples were separated and washed with dH_2O three times. Then, Fe-BS-D, Mn-BS-D, and Fe/Mn-BS-D (or Fe-BS-B, Mn-BS-B, and Fe/Mn-BS-B) were dried at 60°C for 12 h and passed through a 60-mesh sieve. Fig. 1 shows the scanning electron microscopy (SEM) images of Fe/Mn-BS-D and Fe/Mn-BS-B. The basic physico-chemical properties of the tested samples are shown in Table 1.

2.2.3. Influence of environmental factors on antibiotic adsorption

Three environmental factors: temperature, pH, and I were discussed.

The pH of the initial solution was set at 1, 3, 5, 7, and 9.

The I values of the initial solution was set at 0.01, 0.05, 0.1, 0.2, and 0.5 mol/L (at which the pH was best controlled).

The experimental temperatures were set at 10°C, 20°C, 30°C, and 40°C (at which the best pH and I were controlled).

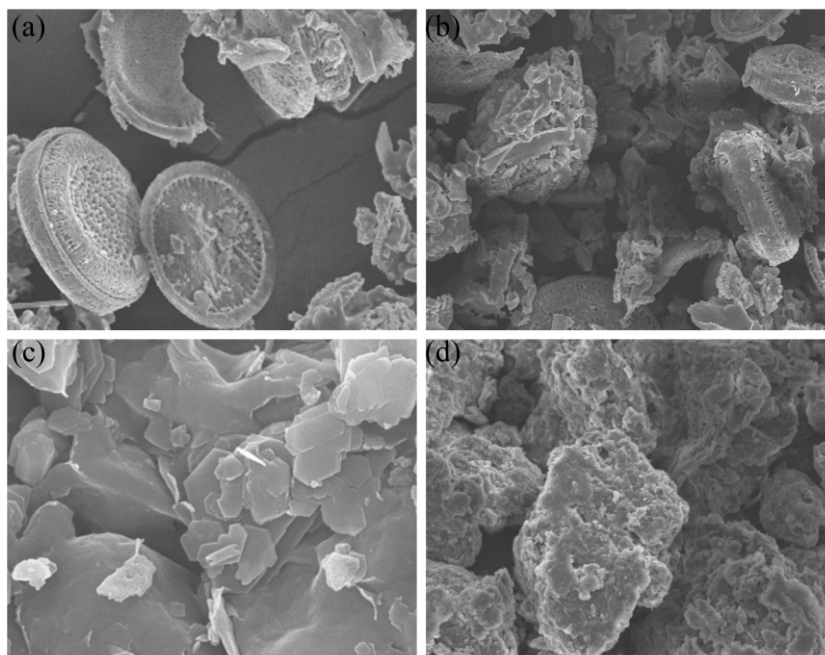


Fig. 1. SEM images of D (a), Fe/Mn-BS-D (b), B (c), and Fe/Mn-BS-B (d).

Table 1
Physico-chemical properties of the tested samples

| Tested sam- ple | pH | Cation exchange capacity (mmol/kg) | Specific surface area (m ² /g) |
|--------------------|-------|---------------------------------------|--|
| D | 7.2 | 330.12 | 67.26 |
| BS-D | 7.4 | 162.58 | 6.37 |
| Fe-BS-D | 6.9 | 183.57 | 76.29 |
| Mn-BS-D | 7.5 | 221.16 | 88.54 |
| Fe/Mn-BS-D | 7.2 | 281.44 | 110.36 |
| B | 10.21 | 1,001.25 | 62.88 |
| BS-B | 8.22 | 552.23 | 7.34 |
| Fe-BS-B | 7.27 | 681.42 | 87.65 |
| Mn-BS-B | 8.84 | 771.92 | 102.42 |
| Fe/Mn-BS-B | 8.39 | 862.18 | 130.53 |

2.2.4. Isothermal adsorption experiment to antibiotics

The initial concentration gradient of three antibiotics was set at 0.5, 1, 2, 5, 10, 20, 30, 40, and 50 mg/L. Each treatment was repeated thrice under the best environmental factors.

2.3. Experimental method

Batch equilibrium method was used for antibiotic adsorption. A total of 0.5000 g of samples was weighed in nine 50 mL plastic centrifuge tubes, and 20.00 mL of an antibiotic solution with different concentration gradients were added to the pipette under optimal environmental conditions (150 rpm and 12 h oscillation) [26]. The equilibrium adsorption of antibiotics in the supernatant was determined through centrifugation at 4,800 rpm for 20 min, the

equilibrium adsorption amount of antibiotics was determined, and the equilibrium adsorption amount of each material was calculated through subtraction.

2.4. Data processing

2.4.1. Calculation of equilibrium adsorption capacity

The equilibrium adsorption capacity of the tested sample for antibiotics was calculated according to Eq. (2):

$$q = \frac{(C_0 - C_e)V}{m} \quad (2)$$

where V is the volume of solution (mL); C_0 is the antibiotic concentration at the starting point (mmol/L); C_e is the antibiotic concentration at the equilibrium point (mmol/L); m is the mass of tested sample (g); and q is the equilibrium adsorption capacity of tested sample for antibiotics (mmol/kg).

2.4.2. Fitting of adsorption isotherms

Based on the adsorption isotherm trend, Langmuir isotherm was selected to fit the antibiotic adsorption isotherm. Eq. (3) was defined as follows:

$$q = \frac{q_m bc}{1 + bc} \quad (3)$$

where q is the equilibrium adsorption amount of antibiotics for the amended soil, mol/kg; c is the equilibrium concentration of antibiotics in the solution, mol/kg; q_m is the maximum adsorption amount of antibiotics for the tested

sample, mol/kg; b is the apparent equilibrium constant of antibiotic adsorption on the tested sample for the measurement of adsorption affinity.

2.4.3. Calculation of thermodynamic parameters

Parameter b in the Langmuir model is equivalent to the apparent adsorption constant of equilibrium constant, and the thermodynamic parameter calculated by $b = K$ or K_a was called the apparent thermodynamic parameter; Eqs. (2)–(4) were defined as follows:

$$\Delta G = -RT \ln K \tag{4}$$

$$\Delta S = \frac{\Delta H - \Delta G}{T} \tag{5}$$

$$\Delta H = R \left(\frac{T_1 \cdot T_2}{T_2 - T_1} \right) \cdot \ln \left[\frac{K_a, T_2}{K_a, T_1} \right] \tag{6}$$

where ΔG is the standard free energy change (kJ/mol), R is a constant (8.3145 J/mol K), T is the adsorption temperature

($T_1 = 293.16$ K, $T_2 = 313.6$ K), ΔH is the enthalpy of adsorption process (kJ/mol), and ΔS is the entropy change of adsorption process (J/mol K).

CurveExpert 1.4 fitting software was used in isothermal fitting, and SigmaPlot 10.0 software was adopted to improve data plotting. SPSS 16.0 statistical analysis software was used to process the experimental data for variance and correlation analysis. SigmaPlot 10.0 software was adopted to improve data plotting. The data were expressed as the means with standard deviation, and different letters indicate significant differences among various amendments. Analysis of variance was performed to determine the effects of amendments, followed by Tukey's honestly significant difference test. Differences of $p < 0.05$ were considered significant.

3. Results and discussion

3.1. Effect of pH on antibiotic adsorption

Fig. 2 shows the difference in antibiotic adsorption among the test soil samples in a pH range of 1–9. Under the same conditions, the three antibiotic in different tested samples had the following order in decreasing adsorption

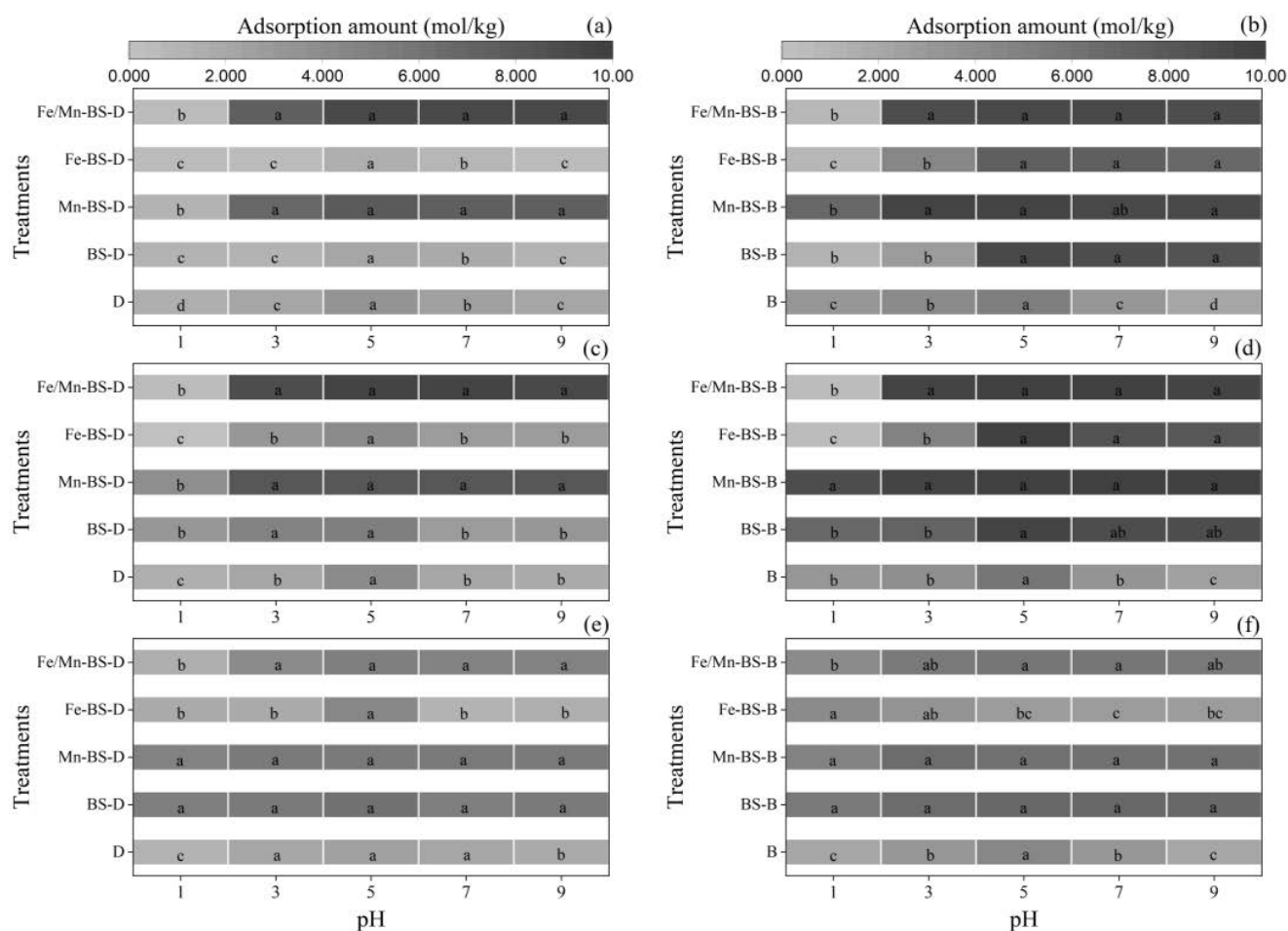


Fig. 2. Influence of pH on the adsorption of CTC (a,b), OTC (c,d), and TC (e,f). Note: Different lowercase letters indicate significant differences between the treatments at the 0.05 level.

capacity: OTC > CTC > TC. With the increase in pH, the adsorption amount of CTC, OTC, and TC increased first and then decreased, and the maximum value was obtained at pH = 5. When pH = 1, the adsorption capacities of CTC, OTC, and TC in different tested samples were low. When pH was changed from 1 to 5, the adsorption amount of antibiotics by the tested samples increased 0.72–17.42 times (CTC), 0.11–25.11 times (OTC), and 0.14–1.09 times (TC). The reason was that under acidic conditions, antibiotics mainly exist in the form of cations. H⁺ in the system competed with the antibiotics on the surfaces of tested samples, hindering the adsorption of antibiotics [27]. As pH increased (pH 1–5), the adsorption ability of antibiotic molecules on a sample surface was gradually enhanced, and the electronegativity

of the sample surface was further enhanced, the surface positive charge of BS-12 adsorbed on clay increased, the surface hydrophilicity of BS-12 decreased, the hydrophobicity of BS-12 increased, and the adsorption of antibiotics by BS-12-modified clay increased [28,29].

3.2. Effect of ionic strength on the adsorption of antibiotics

At the optimal pH (pH = 5), the adsorption amount of the three antibiotics by each test sample decreased with increasing *I* in a range of 0.01–0.5 mol/L (Fig. 3). When *I* = 0.01–0.1 mol/L, the adsorption amount of antibiotics on the test samples slightly decreased, and the decreases were less than 27% (CTC), 21% (OTC), and 15% (TC). At *I* of

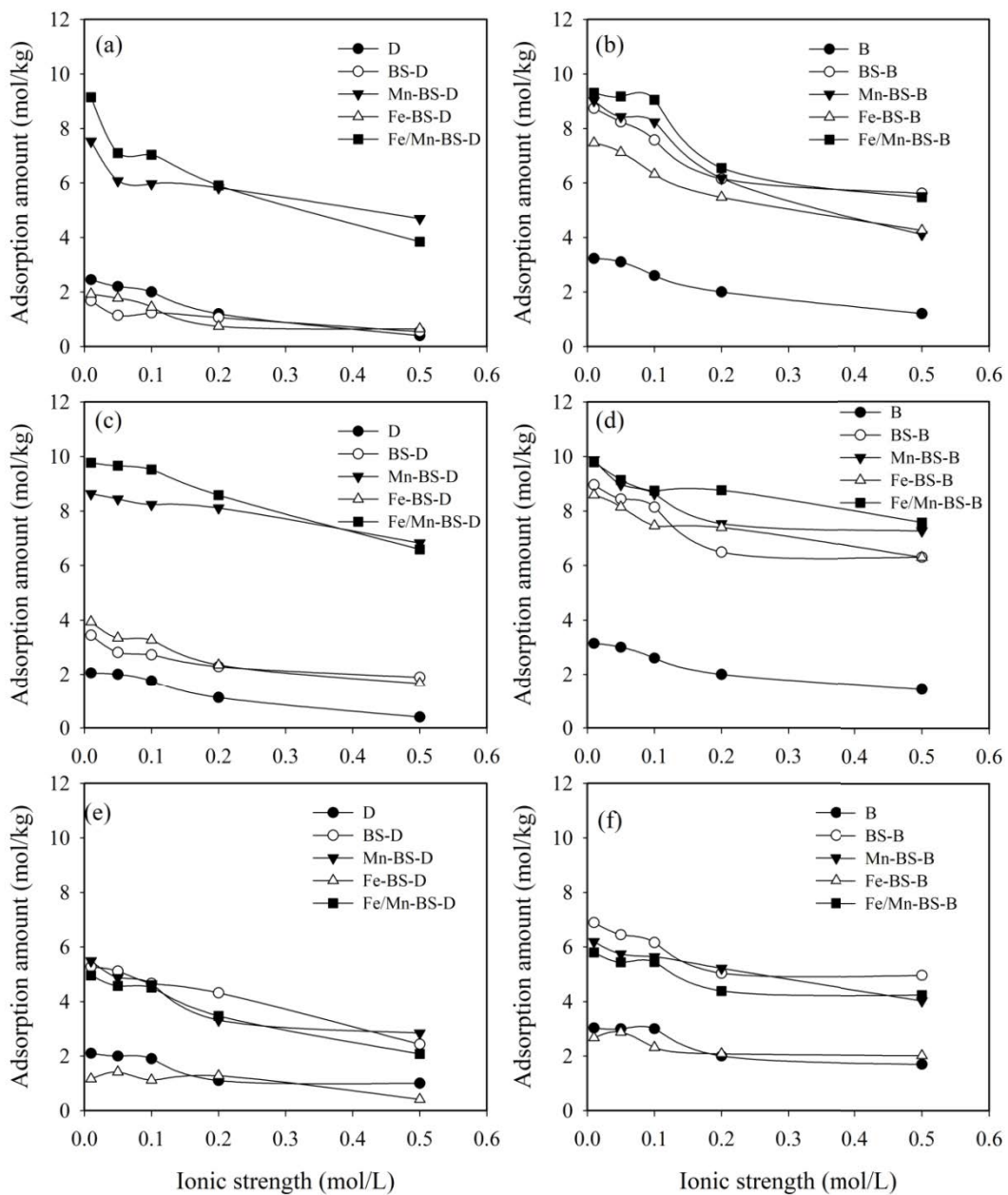


Fig. 3. Effect of ionic strength on the adsorption of CTC (a,b), OTC (c,d), and TC (e,f) at pH = 5.

0.1–0.5 mol/L, the decreases significantly increased, ranging from 15% to 40%. Under the same conditions, the decrease in antibiotic adsorption by different tested samples were ranked in the order of CTC > OTC > TC. The above results may be due to the low concentration of Na⁺ in the solution and the enhanced hydrophobicity of antibiotics, which improved the solubility of the antibiotics. When the concentration of Na⁺ in the solution was high, antibiotic molecules were not easily released, so their solubility was reduced. When Na⁺ was attached to the surfaces of the material samples, the exchange points of the cations of the materials were reduced, and the exchangeable reaction on material samples with antibiotics was reduced [30].

3.3. Effect of temperature on antibiotic adsorption

At pH = 5 and I = 0.01 mol/L, the adsorption amount of the three antibiotics in each test sample increased with the increase in temperature (Fig. 4), showing a positive temperature effect. When the temperature increased from 10°C to 40°C, the increasing amount of antibiotics adsorbed by the tested samples were 0.26–1.92 mol/kg (CTC), 0.46–2.73 mol/kg (OTC), and 0.78–2.02 mol/kg (TC), respectively. The increased amplitudes of the D- and B-based materials were similar. The results showed that at a high temperature, the antibiotics strongly bind to the active sites of the tested samples, consistent with

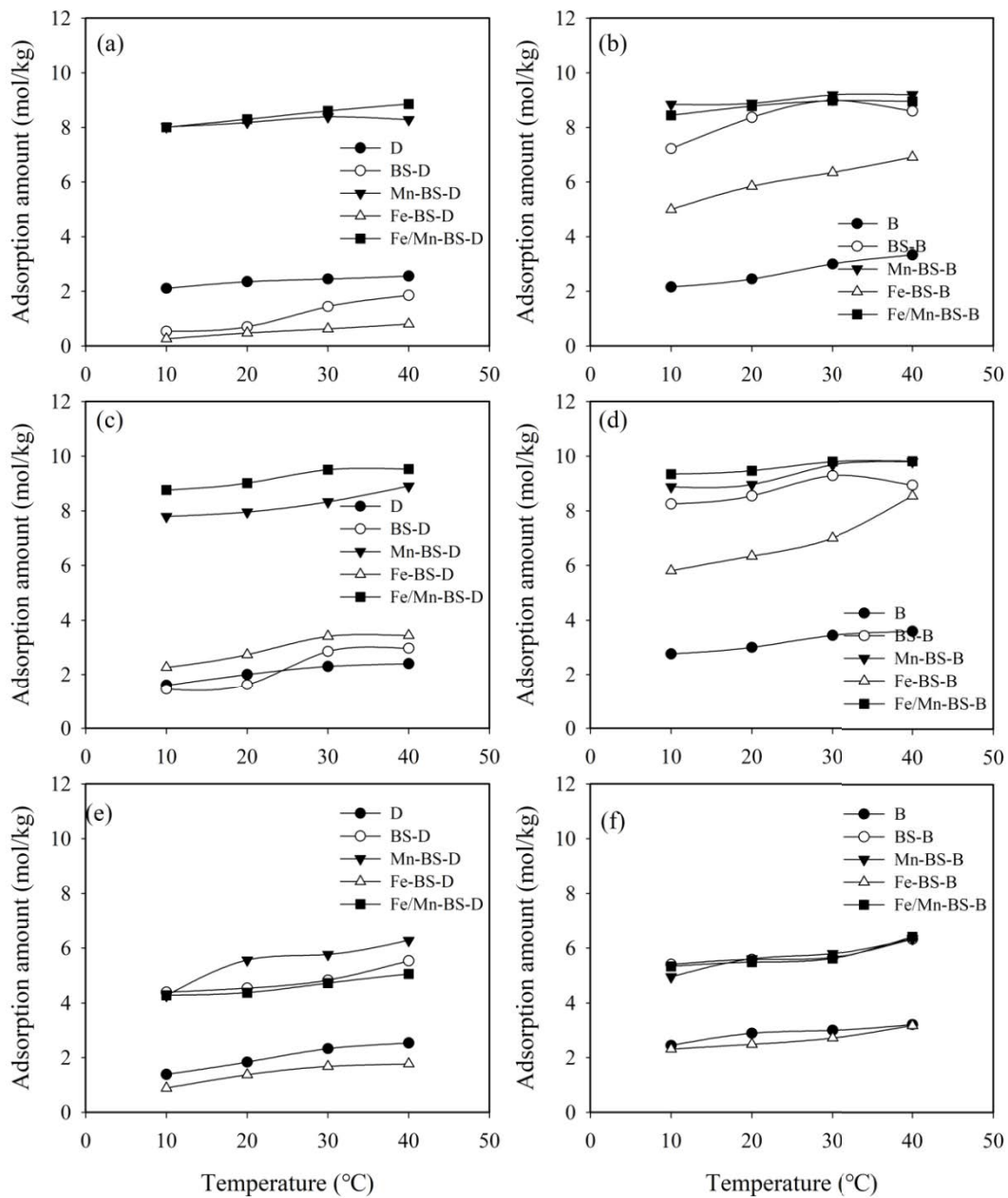


Fig. 4. Adsorption amount of CTC (a,b), OTC (c,d), and TC (e,f) in each soil sample at pH = 5 and I = 0.01 mol/L.

previous studies [31]. As temperature increased, the diffusion velocity of antibiotic molecules in the solution, the contact rate between antibiotics and the surfaces of materials, and the endothermic reaction between antibiotics and the materials surface increased. Increase in temperature also promoted ion exchange and hydrophobic interaction between the antibiotics and materials [22,26].

3.4. Isothermal adsorption characteristics of antibiotics

The adsorption isotherms of antibiotics on each test sample under the most suitable environmental conditions ($\text{pH} = 3$, $I = 0.01 \text{ mol/L}$, and 40°C) are shown in Fig. 5. The adsorption isotherms of the antibiotics on different tested samples were all “L” type. In this experiment, Langmuir adsorption isotherm equation was used to fit the adsorption equilibrium isotherms of antibiotics, and the result parameters are shown in Table 2. The fitting correlation coefficients all reached very significant level ($P < 0.01$), indicating that

the adsorption processes of TC, CTC, and OTC by the tested samples can be described well by the Langmuir model. The maximum adsorption amount (q_m) of antibiotics for each tested sample had ranges of 3.33–21.52 mol/kg (CTC), 3.98–30.26 mol/kg (OTC), and 1.86–11.96 mol/kg (TC), and q_m was ranked in the order of $\text{OTC} > \text{CTC} > \text{TC}$ under the same clay modification conditions. In an antibiotic, the q_m of the tested samples showed the following trend: $\text{BS-Mn-B/D} > \text{BS-Fe/Mn-B/D} > \text{BS-B/B} > \text{BS-Fe-D/B} > \text{D/B}$. The affinity constant b of each tested sample for antibiotic adsorption was maintained in the range of 6.90–188.64, implying a strong adsorption affinity, and the adsorption affinity showed the order $\text{CTC} > \text{OTC} > \text{TC}$.

D (or B) has a high specific surface area and abundant surface adsorption sites and can form a weak ion exchange effect on antibiotics. When D (or B) was modified by BS, BS was easily combined with the negative charge sites on the outer surface of the D (or B) by the positive charge group $-\text{N}^+$ end. The antibiotics were adsorbed through negative

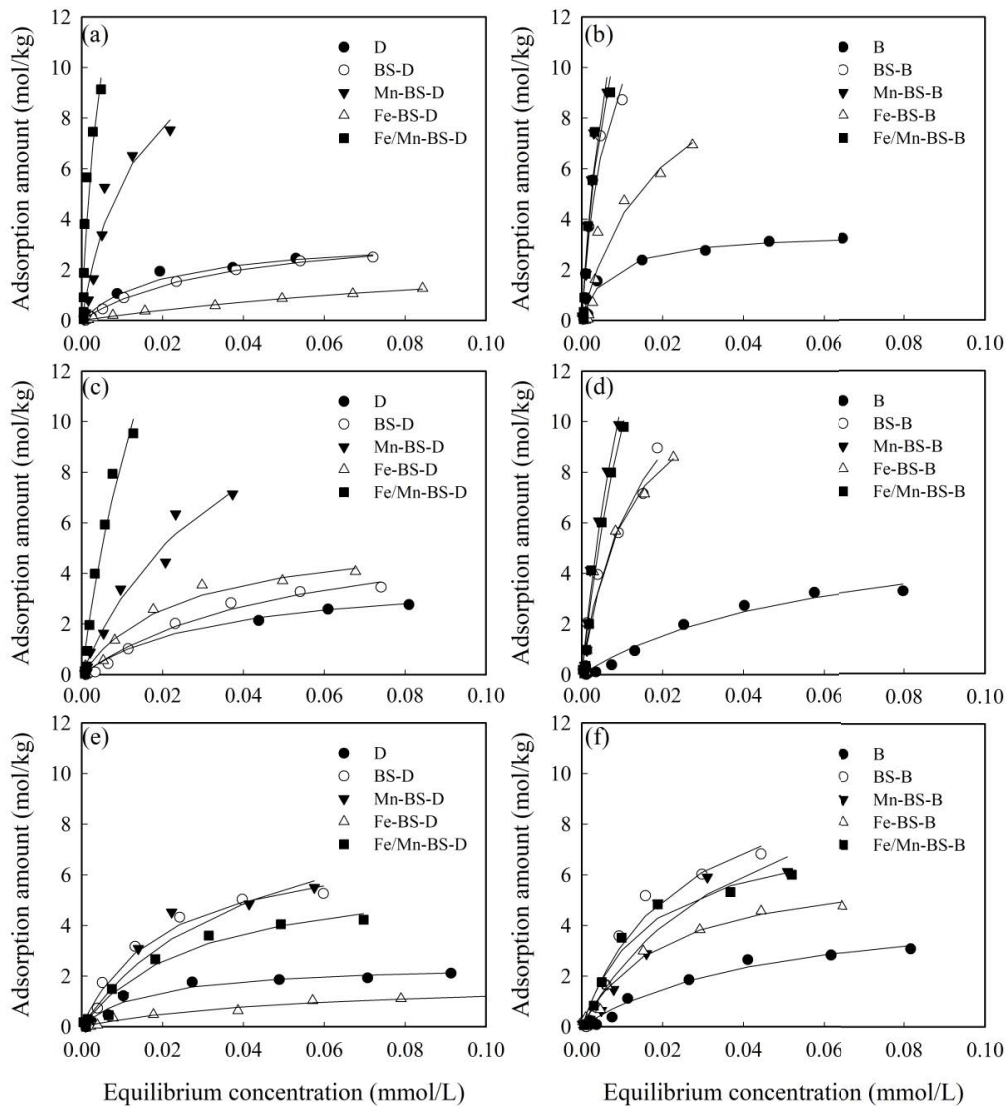


Fig. 5. Adsorption isotherms of each test soil sample to CTC (a,b), OTC (c,d), and TC (e,f).

Table 2
Langmuir parameters of each test soil sample to adsorb antibiotics

| Antibiotic | Tested sample | Correlation coefficient (r) | Standard deviation (S) | q_m (mol/kg) | b (L/mol) |
|------------|---------------|---------------------------------|----------------------------|----------------|-------------|
| CTC | D | 0.9865 ^a | 0.19 | 3.33 | 49.39 |
| | BS-D | 0.998 ^a | 0.06 | 3.80 | 28.49 |
| | Mn-BS-D | 0.9695 ^a | 0.77 | 12.60 | 77.75 |
| | Fe-BS-D | 0.9979 ^a | 0.03 | 3.39 | 6.90 |
| | Fe/Mn-BS-D | 0.9266 ^a | 1.38 | 20.32 | 188.64 |
| | B | 0.9832 ^a | 0.26 | 3.51 | 150.76 |
| | BS-B | 0.9632 ^a | 0.95 | 14.98 | 165.08 |
| | Mn-BS-B | 0.9618 ^a | 0.99 | 21.52 | 129.98 |
| | Fe-BS-B | 0.9607 ^a | 0.80 | 11.65 | 55.02 |
| | Fe/Mn-BS-B | 0.9582 ^a | 0.96 | 19.48 | 138.92 |
| OTC | D | 0.9850 ^a | 0.21 | 3.98 | 29.98 |
| | BS-D | 0.9909 ^a | 0.21 | 6.31 | 18.76 |
| | Mn-BS-D | 0.9863 ^a | 0.49 | 14.42 | 27.18 |
| | Fe-BS-D | 0.9889 ^a | 0.26 | 5.72 | 40.96 |
| | Fe/Mn-BS-D | 0.9774 ^a | 0.82 | 28.76 | 42.30 |
| | B | 0.9878 ^a | 0.23 | 6.20 | 16.76 |
| | BS-B | 0.9813 ^a | 0.69 | 15.13 | 68.79 |
| | Mn-BS-B | 0.9827 ^a | 0.73 | 30.26 | 55.51 |
| | Fe-BS-B | 0.9724 ^a | 0.82 | 12.36 | 97.82 |
| | Fe/Mn-BS-B | 0.9847 ^a | 0.68 | 29.85 | 48.83 |
| TC | D | 0.9817 ^a | 0.18 | 2.50 | 62.60 |
| | BS-D | 0.9855 ^a | 0.40 | 7.50 | 48.09 |
| | Mn-BS-D | 0.9615 ^a | 0.67 | 9.87 | 24.44 |
| | Fe-BS-D | 0.9866 ^a | 0.08 | 1.86 | 18.23 |
| | Fe/Mn-BS-D | 0.9831 ^a | 0.34 | 6.30 | 35.08 |
| | B | 0.9879 ^a | 0.21 | 5.10 | 20.95 |
| | BS-B | 0.9802 ^a | 0.58 | 10.86 | 42.74 |
| | Mn-BS-B | 0.9697 ^a | 0.66 | 11.96 | 24.97 |
| | Fe-BS-B | 0.9938 ^a | 0.23 | 6.51 | 48.67 |
| | Fe/Mn-BS-B | 0.9939 ^a | 0.46 | 8.09 | 60.32 |

Note: ^aindicates that there is a significant correlation at the level of $p = 0.01$. When the degree of freedom $f = 8$ and $p = 0.01$, $r = 0.765$.

charge points, such as the carboxyl group of BS-D (or BS-B) and residual negative charge of D (or B) through ion exchange. Moreover, antibiotics and the long carbon chain of BS-12 formed hydrophobic bonds on the surface of BS-D (or BS-B), and thus the q_m of antibiotics in BS-D (or BS-B) were higher than that of D (or B) [26,27]. After loading by Mn or Fe, the specific surface area and surface adsorption sites of BS-D (or BS-B) improved, and the adsorption capacity of antibiotics by Fe/Mn-BS-D and Fe/Mn-BS-B increased [32]. Compared with the above result, the amphoteric clay-based composite material used in water improvement had a high adsorption capacity for antibiotics and is thus a good improvement material.

3.5. Thermodynamic characteristics on antibiotic adsorption

The results of the thermodynamic parameters of TC, CTC, and OTC adsorption by the tested samples are shown in Table 3. The apparent free energy change ΔG of antibiotic adsorption at 10°C and 40°C was negative, indicating

that the adsorption of antibiotic on all the tested samples were spontaneous. The $\Delta G_{40} > -\Delta G_{10}$, indicating that increase in temperature enhanced the spontaneity of antibiotic adsorption. The apparent enthalpy change ΔH values of antibiotic adsorption on the tested samples were all positive, indicating that the adsorption of antibiotic was endothermic, and increase in temperature enhanced adsorption. These ΔH values were completely consistent with the conclusion about temperature effect and were mutually verified. The ΔS values of the tested samples were positive, indicating that the surface disorder of adsorption system was large. The adsorption of antibiotics on different tested samples was spontaneous, endothermic, and entropy increasing. The above results are consistent with those of Zou et al. [26].

3.6. Effect of physico-chemical properties on antibiotic adsorption

Table 4 shows the linear fitting results between q_m and the physico-chemical properties of different material samples.

Table 3
Thermodynamic parameters of antibiotics adsorbed by each test soil sample

| Antibiotic | Tested sample | ΔG (kJ/mol) | | ΔH (kJ/mol) | ΔS (J/mol K) |
|------------|---------------|---------------------|--------|---------------------|-------------------------|
| | | 10°C | 40°C | | |
| CTC | D | -8.93 | -10.38 | 4.75 | 48.30 |
| | BS-D | -7.26 | -11.25 | 30.40 | 132.99 |
| | Mn-BS-D | -10.20 | -11.37 | 0.79 | 38.83 |
| | Fe-BS-D | -3.14 | -6.39 | 27.55 | 108.40 |
| | Fe/Mn-BS-D | -12.25 | -13.81 | 2.48 | 52.03 |
| | B | -11.51 | -13.86 | 10.64 | 78.22 |
| | BS-B | -11.68 | -13.37 | 4.28 | 56.35 |
| | Mn-BS-B | -11.45 | -12.76 | 0.94 | 43.75 |
| | Fe-BS-B | -9.06 | -10.87 | 7.98 | 60.20 |
| | Fe/Mn-BS-B | -11.52 | -12.90 | 1.44 | 45.76 |
| OTC | D | -7.48 | -9.33 | 9.96 | 61.60 |
| | BS-D | -6.63 | -9.21 | 17.72 | 86.01 |
| | Mn-BS-D | -7.73 | -8.89 | 3.28 | 38.86 |
| | Fe-BS-D | -8.29 | -10.26 | 10.28 | 65.59 |
| | Fe/Mn-BS-D | -8.75 | -9.89 | 2.06 | 38.19 |
| | B | -6.44 | -7.80 | 6.39 | 45.32 |
| | BS-B | -9.88 | -11.13 | 1.95 | 41.78 |
| | Mn-BS-B | -9.43 | -10.69 | 2.40 | 41.78 |
| | Fe-BS-B | -10.58 | -12.71 | 9.49 | 70.88 |
| | Fe/Mn-BS-B | -9.12 | -10.22 | 1.20 | 36.47 |
| TC | D | -9.08 | -11.61 | 14.81 | 84.37 |
| | BS-D | -9.04 | -10.60 | 5.71 | 52.08 |
| | Mn-BS-D | -6.90 | -8.64 | 9.53 | 58.03 |
| | Fe-BS-D | -5.80 | -8.22 | 17.02 | 80.59 |
| | Fe/Mn-BS-D | -8.32 | -9.64 | 4.09 | 43.85 |
| | B | -6.77 | -8.20 | 6.77 | 47.80 |
| | BS-B | -8.76 | -10.11 | 3.95 | 44.89 |
| | Mn-BS-B | -7.28 | -8.70 | 6.16 | 47.48 |
| | Fe-BS-B | -8.97 | -10.76 | 7.89 | 59.54 |
| | Fe/Mn-BS-B | -9.59 | -11.09 | 4.59 | 50.07 |

pH was negatively correlated with q_m and showed a significant correlation with the q_m of B-based materials. The correlation of CEC and q_m was moderate of B-based materials to CTC adsorption and D-based materials to TC adsorption. CEC has a significant correlation with q_m of D based materials to TC adsorption. S_{BET} was negatively and moderately correlated with the q_m of D-based materials to CTC adsorption, also moderate correlated with q_m of D-based materials to OTC adsorption. The above results show that the pH of materials played a key role in determining the adsorption effect of antibiotic on the tested samples. Three ionizable groups were found in the molecular structures of the antibiotics, and the ionization equilibrium constants pK_{a1} , pK_{a2} and pK_{a3} were 3.30–3.57, 7.49–7.69, and 9.44–9.88, respectively. Antibiotic with $pH < 3.30$ is positively charged, that with pH between 3.30 and 7.69 is positively or negatively charged, and that with $pH > 9.50$ exists as an anion [33]. The negatively charged groups of antibiotics, the electronegativity of clay surface, and the negative charge of BS-12 were enhanced at increased pH. These effects

are all unfavorable to the combination of antibiotics and materials.

4. Conclusion

- At increased pH, the amounts of antibiotics adsorbed by the tested samples increased first and then decreased, and the maximum value was obtained at $pH = 5$. The amounts of the three antibiotics adsorbed by each test sample decreased with increasing I in a range of 0.01–0.5 mol/L.
- The adsorption amounts of the three antibiotics in each test sample increased with the increase in temperature. The adsorption of antibiotics on the tested samples was spontaneous, endothermic, and entropy increasing.
- The adsorption processes of TC, CTC, and OTC were described well by the Langmuir model. The q_m of antibiotics were ranked in the following: $OTC > CTC > TC$. The pH of materials played a key role in the determination of the adsorption effects of antibiotic on the tested samples.

Table 4
Linear relationship between q_m and physico-chemical properties of soil samples

| Antibiotic | Clay type | Regression equation | Correlation coefficients (r) | Standard deviations (S) |
|------------|-----------|------------------------------------|------------------------------|-------------------------|
| CTC | D | $q_m = 136.43 - 17.64\text{pH}$ | -0.5342 | 7.42 |
| | | $q_m = 5.55 + 0.01\text{CEC}$ | 0.1215 | 8.72 |
| | | $q_m = 0.39 - 0.12S_{\text{BET}}$ | -0.6091 | 6.92 |
| | B | $q_m = 68.21 - 6.29\text{pH}$ | -0.9475 ^a | 2.63 |
| | | $q_m = 32.78 - 0.02\text{CEC}$ | -0.5762 | 6.72 |
| | | $q_m = 10.69 - 0.05S_{\text{BET}}$ | -0.2958 | 7.85 |
| OTC | D | $q_m = 138.73 - 17.53\text{pH}$ | -0.3925 | 10.92 |
| | | $q_m = 7.06 + 0.02\text{CEC}$ | 0.1368 | 11.76 |
| | | $q_m = 0.81 + 0.16S_{\text{BET}}$ | 0.5988 | 9.51 |
| | B | $q_m = 89.60 - 8.25\text{pH}$ | -0.8193 ^b | 7.16 |
| | | $q_m = 32.78 + 0.02\text{CEC}$ | 0.2869 | 11.95 |
| | | $q_m = 9.89 + 0.11S_{\text{BET}}$ | 0.4888 | 10.89 |
| TC | D | $q_m = 74.73 - 9.55\text{pH}$ | -0.6487 | 2.98 |
| | | $q_m = 12.55 - 0.03\text{CEC}$ | 0.6034 | 3.12 |
| | | $q_m = 7.06 - 0.02S_{\text{BET}}$ | 0.2398 | 3.80 |
| | B | $q_m = 29.69 - 2.47\text{pH}$ | -0.9185 ^a | 1.32 |
| | | $q_m = 19.39 - 0.01\text{CEC}$ | -0.8354 ^b | 1.83 |
| | | $q_m = 9.88 - 0.02S_{\text{BET}}$ | -0.2834 | 3.19 |

Note: ^a and ^b respectively indicate significant correlation at the level of $p = 0.01$ and 0.05 . When degrees of freedom $f = 4$, $p = 0.01$ and 0.05 , $r = 0.917$ and 0.811 .

Acknowledgements

The authors wish to acknowledge and thank the Scientific Research Foundation of State Key Laboratory of Qinba Bio-Resource and Ecological Environment (SXC-2105), the Fundamental Research Funds of Shaanxi University of Technology (SLGRCQD2027) and China West Normal University (18B023), and the financial assistance from the Tianfu Scholar Program of Sichuan Province (2020–17).

Conflict of interests

The authors declare that they have no conflict of interest.

References

- [1] H.-M. Zhang, M.-K. Zhang, G.-P. Gu, Residues of tetracyclines in livestock and poultry manures and agricultural soils from north Zhejiang Province, *J. Ecol. Rural Environ.*, 3 (2008) 69–73.
- [2] Y. Chen, J. Wen, M. Wu, J.-Y. Li, Q. Wang, J. Yin, *In-situ* application of the diffusive gradients in thin film technique in aquaculture ponds for monitoring antibiotics, hormones, and herbicides, *Environ. Sci. Pollut. Res.*, 29 (2021) 21480–21490.
- [3] N. Hemamalini, S.A. Shanmugam, A. Kathirvelpandian, A. Deepak, V. Kaliyamurthi, E. Suresh, A critical review on the antimicrobial resistance, antibiotic residue and metagenomics-assisted antimicrobial resistance gene detection in freshwater aquaculture environment, *Aquacult. Res.*, 53 (2022) 344–366.
- [4] R. Wang, T.-Z. Liu, T. Wang, The fate of antibiotics in environment and its ecotoxicology: a review, *Acta Ecol. Sin.*, 26 (2006) 265–270.
- [5] P. Bhattacharyya, S. Basak, S. Chakrabarti, Advancement towards antibiotic remediation: heterostructure and composite materials, *ChemistrySelect*, 6 (2021) 7323–7345.
- [6] M.B. Ahmed, J.L. Zhou, H.H. Ngo, W. Guo, Md. Abu Hasan Johir, D. Belhaj, Competitive sorption affinity of sulfonamides and chloramphenicol antibiotics toward functionalized biochar for water and wastewater treatment, *Bioresour. Technol.*, 238 (2017) 306–312.
- [7] K.S.D. Premarathna, A.U. Rajapaksha, N. Adassoriya, B. Sarkar, N.M.S. Sirimuthu, A. Cooray, Y.S. Ok, M. Vithanage, Clay-biochar composites for sorptive removal of tetracycline antibiotic in aqueous media, *J. Environ. Manage.*, 238 (2019) 315–322.
- [8] S.S. Rezaei, B. Kakavandi, M. Noorisepehr, A.A. Isari, S. Zabih, P. Bashardoust, Photocatalytic oxidation of tetracycline by magnetic carbon-supported TiO_2 nanoparticles catalyzed peroxydisulfate: performance, synergy and reaction mechanism studies, *Sep. Purif. Technol.*, 258 (2021) 117936–117949.
- [9] M. Kermani, H. Izanloo, R.R. Kalantary, H.S. Barzaki, B. Kakavandi, Study of the performances of low-cost adsorbents extracted from *Rosa damascena* in aqueous solutions decolorization, *Desal. Water Treat.*, 80 (2017) 357–369.
- [10] A.T. Xie, J.Y. Cui, Y.Y. Chen, J.H. Lang, C.X. Li, Y.S. Yan, J.D. Dai, Simultaneous activation and magnetization toward facile preparation of auricularia-based magnetic porous carbon for efficient removal of tetracycline, *J. Alloys Compd.*, 784 (2019) 76–87.
- [11] M.K. Isakovski, J. Beljin, J. Tričković, S. Rončević, S. Maletić, Current state and future perspectives of carbon-based materials in the environment: fate and application, *Recent Pat. Nanotechnol.*, 15 (2020) 183–196.
- [12] H.X. He, W.B. Li, H.Y. Deng, L.P. Ren, Y.F. Zhang, L. Zhu, J. Xie, T. Li, Surface characteristics of a recyclable and efficient adsorption material, *Mater. Lett.*, 256 (2019) 126658, doi: 10.1016/j.matlet.2019.126658.
- [13] H.Y. Deng, W.B. Li, Y. Zheng, X.H. Zhu, Y.Y. Tian, W.X. Yan, Z.F. Meng, G.C. Chen, Study on the enhanced adsorption of Cu^{2+} in different purple soil layers by amphoteric bentonite, *Earth Environ.*, 46 (2018) 403–409.
- [14] W.B. Li, Z.F. Meng, Z. Liu, H.Y. Chen, Q. Wu, S.E. Xu, Chromium(VI) adsorption characteristics of bentonite under different modification patterns, *Pol. J. Environ. Stud.*, 25 (2016) 1075–1083.

- [15] S. Ren, Z.F. Meng, W. Liu, W.B. Li, J. Deng, Characterization and adsorption performance of phenol on amphoteric modified magnetic bentonites, *J. Agro-Environ. Sci.*, 36 (2017) 108–115.
- [16] P.P. Zhao, Z.F. Meng, Y.T. Yang, S.Y. Yang, S. Ren, Q. Wu, B. Li, J.T. Wang, Studies on adsorption characteristics of BS-12 on kaolinite and its affecting factors, *Chin. J. Soil Sci.*, 46 (2015) 1226–1231.
- [17] W.B. Li, S.Y. Yang, Z.F. Meng, X.B. Cui, W. Liu, D. Bai, Secondary modification mechanisms of BS-12 modified bentonite with DTAB and phenanthrene adsorption by combinedly modified bentonite, *J. Agro-Environ. Sci.*, 34 (2015) 1722–1729.
- [18] C. Abesser, R. Robinson, C. Soulsby, Iron and manganese cycling in the storm runoff of a scottish upland catchment, *J. Hydrol.*, 326 (2006) 59–78.
- [19] E.C. Gillispie, S.E. Taylor, N.P. Qafoku, M.F. Hochella Jr., Impact of iron and manganese nano-metal-oxides on contaminant interaction and fortification potential in agricultural systems – a review, *Environ. Chem.*, 16 (2019) 333–347.
- [20] A. Stockdale, W. Davison, Z. Hao, J. Hamilton-Taylor, The association of cobalt with iron and manganese (oxyhydr)oxides in marine sediment, *Aquat. Geochem.*, 16 (2010) 575–585.
- [21] X.G. Zou, W.Y. Lü, Y.L. Wang, F.L. Wang, R.J. Shu, Y.D. Lu, Y.P. Chen, G.G. Liu, Study on adsorption of Pb²⁺ by mesoporous Fe-Mn binary oxide and its mechanisms, *Acta Sci. Circum.*, 38 (2018) 982–992.
- [22] J. Liang, Y.L. Fang, Y. Luo, G.M. Zeng, J.Q. Deng, X.F. Tan, N. Tang, X.M. Li, X.Y. He, C.T. Feng, S.J. Ye, Magnetic nanoferrromanganese oxides modified biochar derived from pine sawdust for adsorption of tetracycline hydrochloride, *Environ. Sci. Pollut. Res.*, 26 (2019) 5892–5903.
- [23] Y.C. Du, L.P. Wang, J.S. Wang, G.W. Zheng, J.S. Wu, H.X. Dai, Flower-, wire-, and sheet-like MnO₂-deposited diatomites: highly efficient adsorbents for the removal of Cr(VI), *J. Environ. Sci.*, 29 (2015) 71–81.
- [24] M.A.M. Khraisheh, Y.S. Al-degs, W.A.M. Mcminn, Remediation of wastewater containing heavy metals using raw and modified diatomite, *Chem. Eng. J.*, 99 (2003) 177–184.
- [25] L.A. Shah, M. das Graça da Silva Valenzuela, M. Farooq, S.A. Khattak, F.R.V. Diaz, Influence of preparation methods on textural properties of purified bentonite, *Appl. Clay Sci.*, 162 (2018) 155–164.
- [26] Y. Zou, H.-y. Deng, M. Li, Y.-h. Zhao, W.-b. Li, Enhancing tetracycline adsorption by riverbank soils by application of biochar-based composite materials, *Desal. Water Treat.*, 207 (2020) 332–340.
- [27] Q.Q. Chai, S.B. Hu, J.W. Liu, D.C. Li, J. Wang, F.J. He, Effects of the organic modification on the attapulgite adsorption for tetracycline antibiotics, *Environ. Monit. Chin.*, 34 (2018) 95–103.
- [28] R. Kerns, S.D. Dong, S. Fukuzawa, J. Carbeck, J. Kohler, L. Silver, D. Kahne, The role of hydrophobic substituents in the biological activity of glycopeptide antibiotics, *J. Am. Chem. Soc.*, 122 (2000) 12608–12609.
- [29] H.Y. Deng, H.X. He, W.B. Li, T. Abbas, Z.F. Liu, Characterization of amphoteric bentonite-loaded magnetic biochar and its adsorption properties for Cu²⁺ and tetracycline, *PeerJ*, 10 (2022) 13030–13049.
- [30] X. Tan, S. Liu, Y. Liu, Y. Gu, G. Zeng, X. Cai, Z.L. Yan, C. Yang, X. Hu, B. Chen, One-pot synthesis of carbon supported calcined-Mg/Al layered double hydroxides for antibiotic removal by slow pyrolysis of biomass waste, *Sci. Rep.-UK*, 6 (2016) 39691–39703.
- [31] Z.C. Li, Q.S. Wei, Z.X. Luo, L.F. Xu, Y.N. Liu, C.Y. Yan, J.S. Liu, Effects of soil and water ratio, pH and organic matter on the adsorption of tetracycline in sediments, *J. Agro-Environ. Sci.*, 36 (2017) 761–767.
- [32] W.B. Li, X.Y. Chen, H.Y. Deng, D. Wang, J.C. Jiang, Y.Z. Zeng, L. Kang, Z.F. Meng, Effects of exogenous biochar on tetracycline adsorption by different riverbank soils from Sichuan and Chongqing section of Jialing river, *Chin. J. Soil Sci.*, 51 (2020) 46–54.
- [33] Z.C. Li, Q.S. Wei, Z.X. Luo, L.F. Xu, Y.N. Liu, C.Z. Yan, J.S. Liu, Combination effects of pH, solution/soil ratio and inherent organic matter on the adsorption of tetracycline by sediments, *J. Agro-Environ. Sci.*, 36 (2017) 761–767.